2024 IEEE International Conference on Robotics and Automation (ICRA 2024)
May 13-17, 2024. Yokohama, Japan

# On Robust Control Laws Trade-off Analysis for Space Manipulators with Uncertain Parameters and Flexible Appendages*

Kostas Nanos, Efstathios Chachamis, and Evangelos Papadopoulos, *Life Fellow, IEEE*

**Abstract. To accurately accomplish on-orbit tasks using Space Manipulator Systems (SMS), advanced model-based controllers, dependent on the knowledge of SMS parameters, can be employed. However, these parameters may change on orbit for several reasons. Also, during an SMS task, excitation of flexible appendages, such as solar panels, or fuel sloshing may introduce significant end-effector errors. Therefore, controllers robust to parametric uncertainty and disturbances are needed. A robust controller attractive due to its small computational effort is the Linear Parameter Varying (LPV) gain-scheduled controller. However, its design for spatial SMS is not trivial and has not been studied yet. Therefore, the aim of this work is to study and compare robust controllers and examine their applicability to SMS. An LPV plus $H_\infty$ controller is compared with a Model-Based PD, and a Model-Based PD plus $H_\infty$ controller, in the presence of parametric uncertainty, noisy measurements and disturbances, using a planar example. The criteria considered include: (i) Design Complexity, (ii) Trajectory Errors, (iii) Required Torques, and (iv) Computational Effort.**

## I. INTRODUCTION

Soon, on-orbit space manipulator systems (SMS), including a spacecraft (S/C) equipped with one or more robotic manipulators, will have a major impact on a wide variety of operations in space, see Fig. 1, [1].

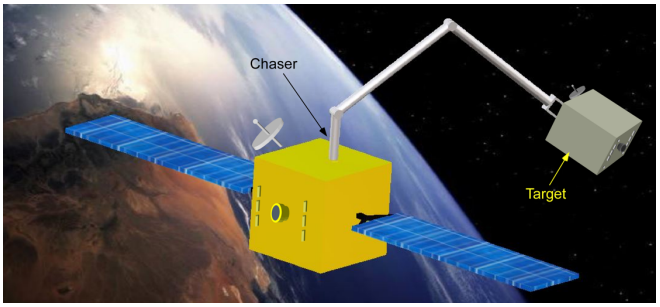


Fig. 1. A space manipulator system (chaser) capturing space object (target).

To accomplish tasks at high accuracy, advanced model-based control strategies which require accurate knowledge of system parameters, can be employed, [2]. However, such parameters may change on orbit for several reasons, such as fuel consumption, deployment of payload, docking to a S/C, or object capture. Robustness in operations, such as on-orbit assembly, maintenance, and repair, refueling, and deorbiting of space debris has always been of significant concern in the design of SMS control algorithms. The Linear Parameter Varying (LPV) gain-scheduled techniques provide a way to apply robust linear control techniques to nonlinear systems with theoretical guarantees of stability and performance. In the last decades, LPV has attracted attention in the fields of unmanned aerial vehicle control (UAVs) [3], and of spacecraft attitude control [4]. However, despite the large number of publications on LPV gain-scheduled methods in the above fields, little work exists on LPV techniques applied to robotic manipulators [5]-[6] and almost negligible number of publications on SMS control [7]. All existing works focus on planar manipulators and rely on certain assumptions to simplify the derivation of the LPV model, limiting their applications to real systems.

In [7], the LPV gain-scheduled control method has been applied on a two-link SMS. A reduced-order LPV model using the parameter set mapping (PSM) algorithm, [6], was obtained, and a LPV state-feedback controller has been designed without considering the effects of parameter uncertainties and/ or disturbances caused by solar panel and slosh fuel motions. The studies focus on control design in the joint space, since in the operational space an increase in the number of scheduling parameters results (i.e., much more complex control design). The operational tasks control problem is addressed indirectly, i.e., using inverse kinematics and then applying joint space control. However, this approach results in large Cartesian errors in the presence of system parameter uncertainties.

The design of LPV controllers for SMS is not a trivial task even for simple planar manipulators since there is no systematic approach for the selection of the appropriate scheduling parameters, limiting their application to real spatial SMS. Assuming a planar SMS, the aim of this work is to study the effectiveness and applicability to realistic systems of the LPV controller against alternative model-based controllers. Therefore, in this paper, an *LPV plus* $H_\infty$ controller is compared to *Model-Based PD* and *Model-Based PD plus* $H_\infty$ controllers considering their robustness to parametric uncertainty, noisy measurements, and disturbances due to solar panel and fuel sloshing. To this end, the criteria employed are: (i) Design Complexity, (ii) Trajectory Errors, (iii) Required Torques, and (iv) Computational Effort.

*This research work was supported by the project "Applied Research for Autonomous Robotic Systems" (MIS5200632) which is implemented within the framework of the National Recovery and Resilience Plan (NNRP) "Greece 2.0" (Measure: 16618- Basic and Applied Research) and is funded by the European Union-NextGenerationEU.
Work done at Athena RC. E. Papadopoulos is with the Robotics Institute, Athena RC, Maroussi 15125, Greece, and with the School of Mechanical Engineering, NTUA. K. Nanos and E. Chachamis are with NTUA/ME. Emails: egpapado@athenarc.gr, [nanos.kostas, stathishahamis]@gmail.com.

## II. Dynamics of Free-Floating SMS

Model-based controllers employ the rigid-body dynamics only, since the addition of flexible appendages (e.g., solar panels) and slosh fuel dynamics results in a very complex model not so useful for control. Moreover, to construct the flexible dynamics model, the estimation of unmeasured variables using nonlinear observers, which complicate the controller design, is required, [8]. Exploiting only the rigid body dynamics in the control design, the avoidance of the solar panels' and/ or slosh fuel flexible modes can be achieved by guidance, providing a desired acceleration profile using pre-shaping techniques, and/ or by selecting appropriate controller gains to achieve a closed-loop response with bandwidth below the flexible appendage and slosh fuel natural frequencies. However, due to parameter uncertainties and the presence of nonlinearities, this may not always be feasible (i.e., some frequencies may be excited).

This study considers an SMS in the *free-floating mode* of operation with *non-zero angular momentum*; this mode is critical in proximity/ capture on-orbit tasks. During this mode, the spacecraft attitude and position are uncontrolled since the spacecraft Attitude Determination and Control System (ADCS) is turned-off to avoid undesired interactions between the spacecraft and manipulator control systems, [9]. The desired manipulator configuration and/ or end-effector position and orientation is achieved by controlling the joint motors via the manipulator control system.

Next, the equations of motion of a rigid-body free-floating SMS (FFSMS) with $N$ joints and non-zero angular momentum are presented briefly. The equations of motions are written in a form suitable for control purposes, [10].

### II.1. *Joint Space Dynamics*

Here, the FFSMS dynamics is written in a form suitable for Joint Space control where the task is to control manipulator joint angles $\mathbf{q}$ applying appropriate joint torques $\boldsymbol{\tau}$ via the manipulator control system. In this case, the dynamics is, [10]

$$\mathbf{H}(\mathbf{q})\ddot{\mathbf{q}}+\mathbf{c}_h(\mathbf{h}_{cm},\boldsymbol{\varepsilon},\eta,\mathbf{q},\dot{\mathbf{q}})+\mathbf{g}_h(\mathbf{h}_{cm},\boldsymbol{\varepsilon},\eta,\mathbf{q})=\boldsymbol{\tau} \tag{1}$$

where $\mathbf{q}$ is the joint angles $N\times 1$ vector, and the spacecraft attitude is defined by spacecraft Euler parameters $\boldsymbol{\varepsilon},\eta$. The column-vector $\boldsymbol{\tau}=[\tau_1,\tau_2,...,\tau_N]^T$ is the manipulator torque vector where $\tau_i$ is the torque applied on the $i^{\text{th}}$ joint. The matrix $\mathbf{H}$ is an $N\times N$ symmetric and positive definite matrix called the *reduced system inertial matrix*, the $N\times 1$ vector $\mathbf{c}_h$ contains the nonlinear Coriolis and centrifugal terms for a spatial FFSMS with non-zero angular momentum $\mathbf{h}_{cm}$, and the vector $\mathbf{g}_h$ is due to the presence of angular momentum and does not vanish for zero joint rates $\dot{\mathbf{q}}$, similarly to the gravity vector in fixed-base manipulators.

### II.2. *Cartesian Space Dynamics*

Here, the dynamics is written in a form suitable for Cartesian Space control where the task is to control the manipulator end-effector pose (position/ attitude) $\mathbf{r}_e$ applying appropriate joint torques $\boldsymbol{\tau}$ via the manipulator control system. The FFSMS dynamics in Cartesian Space is given by, [10]

$$\begin{aligned}&\mathbf{H}_x(\mathbf{q},\boldsymbol{\varepsilon},\eta)\ddot{\mathbf{r}}_e+\mathbf{c}_{h,x}(\mathbf{h}_{cm},\boldsymbol{\varepsilon},\eta,\mathbf{q},\dot{\mathbf{q}},\dot{\boldsymbol{\varepsilon}},\dot{\eta},\dot{\mathbf{r}}_e)\\&+\mathbf{g}_{h,x}(\mathbf{h}_{cm},\boldsymbol{\varepsilon},\eta,\mathbf{q},\dot{\mathbf{q}},\dot{\boldsymbol{\varepsilon}},\dot{\eta})=\mathbf{F}\end{aligned} \tag{2}$$

where $\mathbf{H}_x$ is the *system inertial matrix* in Cartesian space, vector $\mathbf{c}_{h,x}$ contains the nonlinear Coriolis and centrifugal terms for a spatial FFSMS with non-zero angular momentum $\mathbf{h}_{cm}$, the vector $\mathbf{g}_{h,x}$ is due to the angular momentum and

$$\mathbf{F}=\mathbf{J}^{-T}\boldsymbol{\tau} \tag{3}$$

where the matrix $\mathbf{J}$ is an appropriate Jacobian matrix.

## III. Control Strategies

For the selection of the most effective control law under the existence of system parameter uncertainties and disturbances caused by solar panel and/ or slosh fuel motions, a comparison analysis, is performed. The following controllers are considered and compared:

- Model – based PD Controller
- Model – based PD plus $H_\infty$ Controller
- Linear Parameter Varying (LPV) plus $H_\infty$ Controller

The most appropriate controller is selected considering the following criteria:

- Design Complexity
- Trajectory Errors
- Required Torques
- Computational Effort

Next, the design of these controllers is presented briefly.

### III.1. *Model-based PD Controller* (*MB-PD*)

A well-established technique for manipulator control is the *model-based* (or computed torque). It is based on the nominal dynamic model of the manipulator, and essentially it transforms the multivariable nonlinear plant into a set of decoupled linear equations. The model-based controller is attractive because of its simple and elegant mathematical derivation and for providing excellent control performance in the absence of modelling errors and external disturbances. Then, this control law is described by

$$\boldsymbol{\tau}=\hat{\mathbf{H}}(\mathbf{q})\mathbf{u}+\hat{\mathbf{c}}_h(\mathbf{h}_{cm},\boldsymbol{\varepsilon},\eta,\mathbf{q},\dot{\mathbf{q}})+\hat{\mathbf{g}}_h(\mathbf{h}_{cm},\boldsymbol{\varepsilon},\eta,\mathbf{q}) \tag{4}$$

where $\hat{(\cdot)}$ denotes the estimated value of $(\cdot)$ and $\mathbf{u}$ is a new control input to the system.

In case of the *model-based PD controller*, the control input $\mathbf{u}$ has the form,

$$\mathbf{u}=\ddot{\mathbf{q}}_d+\mathbf{K}_D(\dot{\mathbf{q}}_d-\dot{\mathbf{q}})+\mathbf{K}_P(\mathbf{q}_d-\mathbf{q}) \tag{5}$$

where $(\cdot)_d$ denotes the desired value of variable $(\cdot)$.

The controller gains $\mathbf{K}_P$ and $\mathbf{K}_D$ are positive definite diagonal matrices with elements $k_{p,i}$ and $k_{d,i}$, respectively,

$$k_{p,i}=\omega_{n,i}^2,\ k_{d,i}=2\zeta_i\omega_{n,i} \tag{6}$$

where $\zeta_i$ is the desired damping coefficient and $\omega_{n,i}$ is the desired closed – loop system bandwidth.

The closed – loop error dynamics is,

$$\ddot{\mathbf{e}}+\mathbf{K}_D\dot{\mathbf{e}}+\mathbf{K}_P\mathbf{e}=\mathbf{d}+\mathbf{d}_{\text{unc}} \tag{7}$$

where $\mathbf{e}=\mathbf{q}_d-\mathbf{q}$ is the error in Joint Space, the term $\mathbf{d}$ represents the disturbances due to the unmodelled flexible dynamics (e.g., solar panels, fuel sloshing, etc.) and

$$\mathbf{d}_{\mathbf{unc}}=\hat{\mathbf{H}}^{-1}\left[(\mathbf{H}-\hat{\mathbf{H}})\ddot{\mathbf{q}}+(\mathbf{c}_h-\hat{\mathbf{c}}_h)+(\mathbf{g}_h-\hat{\mathbf{g}}_h)\right] \tag{8}$$

is a term due to the parametric uncertainty and acts as a disturbance to the closed loop system formed by the model-based controller.

Moreover, since in practice the computation of the vector $\hat{\mathbf{c}}_h$ contributes mostly to the controller computational effort, one can assume $\hat{\mathbf{c}}_h=\mathbf{0}$. This assumption contributes to the term $\mathbf{d}_{\mathbf{unc}}$ like parameter uncertainties. If we had perfect knowledge of the system parameters and dynamics, the term $\mathbf{d}_{\mathbf{unc}}$ would vanish.

Note that if the controller gains selected are relatively large and the closed – loop system bandwidth $\omega_{n,i}$ becomes comparable to the unmodelled flexible dynamics, then, an undesired oscillatory behavior may result leading even to system instability. To avoid such phenomena, the closed – loop system bandwidth $\omega_{n,i}$ must be selected at least two times (ideally five times) below the lowest resonant frequency $\omega_{res}$ of the system flexible dynamics, i.e.,

$$\omega_{n,i}<1/2\cdot\omega_{res} \tag{9}$$

where

$$\omega_{res}=\min(\omega_{panel},\omega_{slosh}) \tag{10}$$

where $\omega_{panel}$, $\omega_{slosh}$ are the lowest resonant frequencies due to panel and slosh fuel motions, respectively.

Considering the beam theory for the solar panel motion, [11], and assuming a spring – damper model for the slosh fuel motion, these lowest resonant frequencies are given by,

$$\omega_{panel}=3.516\left(\frac{EI}{\sigma L^4}\right)^{1/2},\ \omega_{slosh}=\left(\frac{k_{slosh}}{m_{slosh}}\right)^{1/2} \tag{11}$$

where $E$ is Young's modulus of elasticity, $I$ is the cross - sectional area moment of inertia, $L$ is the length, $\sigma$ is the mass density per length (kg/m) of the solar panel and $m_{slosh}$, $k_{slosh}$ are the slosh fuel mass and the slosh fuel equivalent spring constant, respectively. Note that one should consider that in practice, both frequencies are estimated with some uncertainty, [12].

Regarding the Cartesian Space control, the design procedure is similar to that of the Joint Space control considering the Cartesian Space dynamics, i.e., (2), instead of Joint Space dynamics, i.e., (1).

III.2. *Model-based PD Plus $H_\infty$ Controller* (*MB-PD/ $H_\infty$*)

In the presence of parameter uncertainty and nonlinearities, the avoidance of the excitation of solar panels and/or slosh fuel flexible modes, may not be feasible always (i.e., some frequencies may be excited), even if precautions such as the above are taken, especially since the lowest resonant frequency is subject to uncertainties. Therefore, parameter uncertainties and disturbances, caused by solar panel and slosh fuel motions, may degrade considerably the performance achievable by a model-based PD controller. Nevertheless, this can be overcome by adding a linear robust $H_\infty$ action to the model-based PD. Then, the control law is given by, [13]

$$\boldsymbol{\tau}=\hat{\mathbf{H}}\mathbf{u}+\hat{\mathbf{c}}_h+\hat{\mathbf{g}}_h-\hat{\mathbf{H}}\mathbf{u}_\infty \tag{12}$$

where $\mathbf{u}_\infty$ is the $H_\infty$ contribution to the controller and the input $\mathbf{u}$ is given by the (5).

The design of the robust controller is performed in two steps. First, the model-based part of the controller is used to pre-compensate the dynamics of the nominal system. Then, the $H_\infty$ controller is used to post-compensate the residual error which is not completely removed by the model-base part of the controller.

In this case, the closed – loop system error dynamics is,

$$\ddot{\mathbf{e}}+\mathbf{K}_D\dot{\mathbf{e}}+\mathbf{K}_P\mathbf{e}=\mathbf{d}+\mathbf{d}_{\mathbf{unc}}+\mathbf{u}_\infty \tag{13}$$

where the diagonal elements of the controller gains $\mathbf{K}_P$ and $\mathbf{K}_D$ are given by (6). To avoid flexible modes excitation, the closed-loop system frequency $\omega_{n,i}$ is selected by (9).

It is desired that the right-hand side of (13) is zero. This is feasible if $\mathbf{u}_\infty$ cancels $\mathbf{d},\mathbf{d}_{\mathbf{unc}}$ for all time.

To design the linear $H_\infty$ control law, the terms $\mathbf{d},\mathbf{d}_{\mathbf{unc}}$ are temporarily ignored and (13) is written as,

$$\ddot{\mathbf{e}}+\mathbf{K}_D\dot{\mathbf{e}}+\mathbf{K}_P\mathbf{e}=\mathbf{u}_\infty \tag{14}$$

The above equation can be represented in state - space as,

$$\dot{\mathbf{E}}=\mathbf{A}\mathbf{E}+\mathbf{B}\mathbf{u}_\infty \tag{15}$$

and

$$\mathbf{y}=\mathbf{E}=\mathbf{C}\mathbf{E}+\mathbf{D}\mathbf{u}_\infty \tag{16}$$

where

$$\mathbf{E}=[\mathbf{e}^T\quad\dot{\mathbf{e}}^T]^T \tag{17}$$

and

$$\mathbf{A}=\begin{bmatrix}\mathbf{0}_{\mathrm{N}\times\mathrm{N}} & \mathbf{I}_{\mathrm{N}}\\ -\mathbf{K}_P & -\mathbf{K}_D\end{bmatrix},\ \mathbf{B}=\begin{bmatrix}\mathbf{0}_{\mathrm{N}\times\mathrm{N}}\\ \mathbf{I}_{\mathrm{N}}\end{bmatrix}$$
$$\mathbf{C}=\begin{bmatrix}\mathbf{I}_{\mathrm{N}} & \mathbf{0}_{\mathrm{N}\times\mathrm{N}}\\ \mathbf{0}_{\mathrm{N}\times\mathrm{N}} & \mathbf{I}_{\mathrm{N}}\end{bmatrix},\ \mathbf{D}=\begin{bmatrix}\mathbf{0}_{\mathrm{N}\times\mathrm{N}}\\ \mathbf{0}_{\mathrm{N}\times\mathrm{N}}\end{bmatrix} \tag{18}$$

where $\mathbf{0}_{m\times n}$ is the $m\times n$ zero matrix and $\mathbf{I}_k$ is the $k\times k$ identity matrix.

The design variables of the $H_\infty$ controller are the $N\times N$ matrices $\mathbf{W}_\mathbf{u}(s)$, $\mathbf{W}_\mathbf{di}(s)$ and the $2N\times 2N$ matrices $\mathbf{W}_\mathbf{e}(s)$ and $\mathbf{W}_\mathbf{n}(s)$ which are called *weighting functions*. Each one can be expressed as a diagonal matrix of transfer functions or static gains and has its own objective.

The control weighting function $\mathbf{W}_\mathbf{u}(s)$ is applied to the control input. Typically, this is a *high-pass filter* applied to each input and used to reduce the control effort $\mathbf{u}$. The performance weighting function $\mathbf{W}_\mathbf{e}(s)$ is applied to the error of the closed-loop system. It can be a mix of low-pass filters and static gains and is used to shape the system's performance. Therefore, the main aim of the performance and control weighting functions is to shape the response so that the gain of the loop transfer function $L=GK$ is high at a lower frequency range and low at a higher frequency range. The weighting function $\mathbf{W}_\mathbf{di}(s)$ is used to model the type of disturbances $\mathbf{d}_\mathbf{i}$ (including those caused by system

uncertainties) and the function $\mathbf{W_n}(s)$ is used to model the expected sensor noise $\mathbf{n}$. Typically, functions $\mathbf{W_{di}}(s)$ and $\mathbf{W_n}(s)$ are diagonal matrices, with their diagonal elements represented by low-pass and high-pass filters, respectively. Some standard guidelines propose that matrices $\mathbf{W_u}(s)$ and $\mathbf{W_e}(s)$ may have the following form, [14],

$$\mathbf{W_u}(s)=\left(\frac{s+\omega_{bc}/\sqrt[k]{M_u}}{\sqrt[k]{\varepsilon_1}\,s+\omega_{bc}}\right)^k\cdot\mathbf{I_N},\ k\geq 1 \tag{19}$$

$$\mathbf{W_e}(s)=\left(\frac{s/\sqrt[k]{M_s}+\omega_b}{s+\omega_b\sqrt[k]{\varepsilon}}\right)^k\cdot\mathbf{I_{2N}},\ k\geq 1 \tag{20}$$

where $M_s=\|\mathbf{S}\|_\infty$ is the peak of the Sensitivity Function $\mathbf{S}$, $\omega_b$ is the desired closed-loop bandwidth, $\varepsilon$ is the desired steady state error with respect to a step input, $M_u$ is the maximum gain measured by $\|\mathbf{KS}\|_\infty$, $\omega_{bc}$ is the controller's bandwidth, $\varepsilon_1$ is a small real number, $k$ is a positive integer that determines the roll-off rate of the closed – loop system and $\|(\cdot)\|_\infty$ indicates the $H_\infty$ norm of $(\cdot)$.

Regarding the Cartesian Space control, the design procedure is similar to that of the Joint Space control considering the Cartesian Space dynamics, i.e., (2), instead of Joint Space dynamics, i.e., (1).

### III.3. *LPV plus $H_\infty$ Control Law (LPV/ $H_\infty$)*

In this section, the $H_\infty$ approach for a LPV system is applied to the FFSMS described by (1). An LPV system can be described by the following state-space model in which the *scheduling parameter* vector $\boldsymbol{\rho}$ is a function of the state vector $\mathbf{x}$, named *quasi-LPV* representation, [6]

$$\dot{\mathbf{x}}=\mathbf{A}(\boldsymbol{\rho}(\mathbf{x}))\mathbf{x}+\mathbf{B}(\boldsymbol{\rho}(\mathbf{x}))\mathbf{u} \tag{21}$$

$$\mathbf{y}=\mathbf{C}(\boldsymbol{\rho}(\mathbf{x}))\mathbf{x}+\mathbf{D}(\boldsymbol{\rho}(\mathbf{x}))\mathbf{u} \tag{22}$$

The scheduling parameter vector $\boldsymbol{\rho}(\mathbf{x}(t))$ is assumed to be measurable and restricted to a set of admissible trajectories based on operating conditions of the system.

Next, the nonlinear dynamics of the FFSMS can be represented as a quasi-LPV system. First, the equations of motion, (1), are written as:

$$\ddot{\mathbf{q}}=-\mathbf{H}^{-1}(\mathbf{q})\mathbf{c}_h(\mathbf{h}_{cm},\boldsymbol{\varepsilon},\eta,\mathbf{q},\dot{\mathbf{q}})-\mathbf{H}^{-1}(\mathbf{q})\mathbf{g}_h(\mathbf{h}_{cm},\boldsymbol{\varepsilon},\eta,\mathbf{q})+\mathbf{u} \tag{23}$$

where

$$\mathbf{u}=\mathbf{H}^{-1}(\mathbf{q})\boldsymbol{\tau} \tag{24}$$

Therefore, defining the state vector as,

$$\mathbf{x}=[\mathbf{q}^T\quad\dot{\mathbf{q}}^T]^T \tag{25}$$

one can write,

$$\dot{\mathbf{x}}=\begin{bmatrix}\dot{\mathbf{q}}\\ \ddot{\mathbf{q}}\end{bmatrix}=\begin{bmatrix}\dot{\mathbf{q}}\\ -\mathbf{H}^{-1}\mathbf{c}_h\end{bmatrix}+\begin{bmatrix}\mathbf{0}_{\mathbf{N}\times 1}\\ -\mathbf{H}^{-1}\mathbf{g}_h\end{bmatrix}+\begin{bmatrix}\mathbf{0}_{\mathbf{N}\times\mathbf{N}}\\ \mathbf{I_N}\end{bmatrix}\mathbf{u} \tag{26}$$

In case there is a scheduling parameter vector $\boldsymbol{\rho}(\mathbf{x})=[\rho_1,\cdots,\rho_l]^T$ which satisfies,

$$\begin{bmatrix}\dot{\mathbf{q}}\\ -\mathbf{H}^{-1}\mathbf{c}_h\end{bmatrix}+\begin{bmatrix}\mathbf{0}_{\mathbf{N}\times 1}\\ -\mathbf{H}^{-1}\mathbf{g}_h\end{bmatrix}=\mathbf{A}(\boldsymbol{\rho}(\mathbf{x}))\mathbf{x} \tag{27}$$

then the FFSMS dynamics, described by (26), can be represented in the following quasi-LPV form:

$$\dot{\mathbf{x}}=\mathbf{A}(\boldsymbol{\rho}(\mathbf{x}))\mathbf{x}+\mathbf{B}\mathbf{u} \tag{28}$$

where

$$\mathbf{B}=[\mathbf{0}_{\mathbf{N}\times\mathbf{N}}\quad\mathbf{I_N}]^T \tag{29}$$

and

$$\mathbf{A}(\boldsymbol{\rho}(\mathbf{x}))=\sum_{i=1}^{l}\rho_i(\mathbf{x})\mathbf{A}_i \tag{30}$$

where $l$ is the number of the scheduling parameters and $\mathbf{A}_i$ is a constant matrix.

The controller design requires *off-line* and *on-line* calculations. If the quasi-LPV form of system requires $l$ scheduling parameters, there are $2^l$ vertices $\Pi_i$ (i=1,.., $2^l$). For each of the vertices $\Pi_i$, a $H_\infty$ control law *i* is designed off-line, i.e.,

$$\dot{\mathbf{x}}_{c,i}=\mathbf{A}_i(\Pi_i)\mathbf{x}_{c,i}+\mathbf{B}_i(\Pi_i)\mathbf{y}_i \tag{31}$$

$$\mathbf{u}_i=\mathbf{C}_i(\Pi_i)\mathbf{x}_{c,i}+\mathbf{D}_i(\Pi_i)\mathbf{y}_i \tag{32}$$

where $\mathbf{y}_i$ is the controller input (e.g., joint error), $\mathbf{u}_i$ is the controller command, and $\mathbf{x}_{c,i}$ is the state vector that describes the controller dynamics.

Each of the $2^l$ controllers, can be written in the following compact form,

$$\mathbf{K}_{\Pi_i}=\begin{bmatrix}\mathbf{A}_i(\Pi_i) & \mathbf{B}_i(\Pi_i)\\ \mathbf{C}_i(\Pi_i) & \mathbf{D}_i(\Pi_i)\end{bmatrix} \tag{33}$$

The final controller is given by,

$$\dot{\mathbf{x}}_c=\mathbf{A}_c(\rho)\mathbf{x}_c+\mathbf{B}_c(\rho)\mathbf{y} \tag{34}$$

$$\mathbf{u}=\mathbf{C}_c(\boldsymbol{\rho})\mathbf{x}_c+\mathbf{D}_c(\boldsymbol{\rho})\mathbf{y} \tag{35}$$

where

$$\begin{bmatrix}\mathbf{A}_c(\boldsymbol{\rho}) & \mathbf{B}_c(\boldsymbol{\rho})\\ \mathbf{C}_c(\boldsymbol{\rho}) & \mathbf{D}_c(\boldsymbol{\rho})\end{bmatrix}=\sum_{i=1}^{2^l}a_i\begin{bmatrix}\mathbf{A}_i(\Pi_i) & \mathbf{B}_i(\Pi_i)\\ \mathbf{C}_i(\Pi_i) & \mathbf{D}_i(\Pi_i)\end{bmatrix} \tag{36}$$

where the coefficients $a_i$ results by *on-line* measurements (or estimation) of the parameters $\boldsymbol{\rho}(\mathbf{x})$, using the following equations,

$$\boldsymbol{\rho}=a_1\Pi_1+a_2\Pi_2+\ldots+a_{2^l}\Pi_{2^l} \tag{37}$$

and

$$\sum_{i=1}^{2^l}a_i=1 \tag{38}$$

The required joint torques are given by (24), i.e.,

$$\boldsymbol{\tau}=\mathbf{H}(\mathbf{q})\mathbf{u} \tag{39}$$

Note that, contrary to the design of model-based PD and model-based PD plus $H_\infty$ controllers, the design of an LPV controller in Cartesian Space is not straightforward and rather too complicated, since the Cartesian Space dynamics must be considered in the LPV representation given by (21).

## IV. Control Schemes Comparison

For the trade-off analysis, the controllers considered are applied to a planar space manipulator system with 2 joints, shown in Fig. 2. Here, the task is the accurate trajectory following of the manipulator angles in joint space despite possible parameter uncertainties, noisy measurements, and disturbances due to S/C solar panel and sloshing. The joint

measurements noise is defined according to [15] - [16]. The manipulator desired trajectories are given by,

$$q_1(t)=q_1^{in}+s(t)(q_1^{fin}-q_1^{in}),q_2(t)=q_2^{in}+s(t)(q_2^{fin}-q_2^{in}) \quad (40)$$

where $[q_1^{in}\ q_2^{in}]=[-15^o\ 60^o]$, $[q_1^{fin}\ q_2^{fin}]=[80^o\ 100^o]$ and $s$ is the arc length parameterization of the path ( $0\le s\le 1$),

$$s(t)=a_0+a_1t+a_2t^2+a_3t^3+a_4t^4+a_5t^5 \quad (41)$$

with initial and final values $s_{in}=0$ and $s_{fin}=1$ respectively and zero initial and final velocities and accelerations.

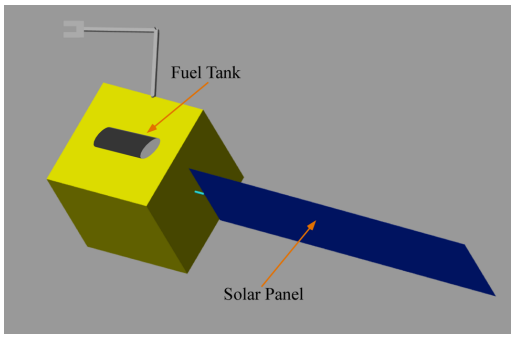


Fig. 2. A planar FFSMS as a SimScape model.

The parameters of the system are presented in Table I. A solar panel is mounted on the S/C. The values of the solar panel parameters are displayed in Table II. The slosh fuel mass is $m_{slosh}=50Kg$, the slosh fuel equivalent spring constant and damping are $k_{slosh}=0.41Nm$ and $c_{slosh}=0.02Nms$, respectively.

TABLE I. PARAMETERS OF THE FFSMS SHOWN IN FIG. 2.

| *Body* | $m_i$ (kg) | $r_i$ (m) | $l_i$ (m) | $I_i$ (kg m$^2$) |
|---|---|---|---|---|
| 0 | 2000 | 1.5 | - | 2250 |
| 1 | 50 | 1.0 | 1.0 | 16.66 |
| 2 | 50 | 1.0 | 1.0 | 16.66 |

TABLE II. PROPERTIES OF THE S/C SOLAR PANEL.

| $E$ (N/m$^2$) | $\rho$ (kg/m$^3$) | $L$ (m) | $W$ (m) | $H$ (m) |
|---|---|---|---|---|
| 71*10$^9$ | 2700 | 7.5 | 1.5 | 0.04 |

In Table II, $\rho$ is the material density, $W$ is the panel width and $H$ is the panel thickness. Here, an uncertainty of the order of 20% in all SMS parameters is considered in the design of the controllers under consideration.

IV.1. *MB-PD Controller Design*

Since only the rigid-body dynamics is considered, the avoidance of solar panel and/or slosh fuel flexible modes excitation can be achieved by selecting appropriate controller gains with bandwidth $\omega_n$ kept below the lowest estimated resonant frequency $\omega_{res}$ of the system flexible dynamics, see (9).

The lowest resonant frequencies $\omega_{panel}$, $\omega_{slosh}$ are given by (11),

$$\omega_{panel}=0.0917rad/s,\ \omega_{slosh}=0.0906rad/s \quad (42)$$

Therefore, (10) results in,

$$\omega_{res}=0.0906rad/s \quad (43)$$

Considering (9), we select,

$$\omega_{n,i}=\frac{1}{2}\omega_{res}=0.0453rad/s \quad (44)$$

Considering a critically damping desired response, i.e., $\zeta_i=1$, the controller gains $\mathbf{K}_P$ and $\mathbf{K}_D$ are:

$$\mathbf{K}_P=0.002\mathbf{I}_2,\mathbf{K}_D=0.0906\mathbf{I}_2 \quad (45)$$

IV.2. *MB-PD/ $H_\infty$ Controller Design*

In case some frequencies are excited during the application of model-based PD controller, despite the design proposed above, an additional $H_\infty$ controller term in the model-based PD formulation can be added to mitigate the effect of the controlled manipulator motion on flexible/oscillatory elements. The PD controller gains are designed as mentioned above. In practice, to avoid computational complexity, we assume $\hat{\mathbf{c}}_h=\mathbf{0}$ in (12). This assumption contributes to the term $\mathbf{d}_{\mathbf{unc}}$, and can be canceled using the $H_\infty$ controller by the selection of appropriate weighting functions. The $H_\infty$ controller is designed using these weighting functions as inputs in Matlab function "*hinfsyn*". For the $H_\infty$ linear controller term the following weighting functions, corresponding to low and high pass filters, are selected by trade-off analysis,

$$\mathbf{W_u}=1000\frac{s+5}{s+50}\mathbf{I}_2,\mathbf{W_e}=1000\frac{0.0001s+1}{0.5s+1}\mathbf{I}_4 \quad (46)$$

$$\mathbf{W_d}=1000\mathbf{I}_2,\mathbf{W_n}=1000\frac{s+10}{s+100}\mathbf{I}_4 \quad (47)$$

IV.3. *LPV/ $H_\infty$ Controller Design*

Regarding the design of the LPV controller, it can be shown that the dynamics, i.e., (1) of a planar FFMS with two joints and non-zero angular momentum can be written in a quasi-LPV form, i.e., (28), where:

$$\mathbf{A}(\boldsymbol{\rho})=\begin{bmatrix}0&0&1&0\\0&0&0&1\\\rho_1(\mathbf{x})&\rho_2(\mathbf{x})&\rho_3(\mathbf{x})&\rho_4(\mathbf{x})\\\rho_5(\mathbf{x})&\rho_6(\mathbf{x})&\rho_7(\mathbf{x})&\rho_8(\mathbf{x})\end{bmatrix},\mathbf{B}=\begin{bmatrix}\mathbf{0}_{2\times2}&\mathbf{I}_2\end{bmatrix}^T \quad (48)$$

where the vector $\boldsymbol{\rho}=[\rho_1\cdots\rho_8]^T$ of scheduling variables is function of state variables $\mathbf{x}=[q_1\ q_2\ \dot{q}_1\ \dot{q}_2]^T$, whose expression is omitted here due to space constraints.

A system reduction is required since for LPV controller design, as the number $N_l$ of linear matrix inequalities (LMIs) to be solved increases exponentially with the number $l$ of scheduling parameters according to $N_l=2^{l+1}+1$. The system reduction may depend on the manipulator desired task. Thus, *different* controllers may be required for a set of desired trajectories making themselves hard to satisfy high performance requirements for SMS in multiple tasks.

Here, the joint trajectories given by (40) are considered and a reduced-order LPV model using the parameter set mapping (PSM) algorithm, proposed in [6], is obtained. Then the singular values are obtained through following the process of LPV reduction and applying PSM to normalize a data matrix. The number of significant singular values is selected

as $m$ = 4 by weighing the accuracy and complexity of reduced LPV model. The final weighting functions are selected by trade-off analysis and are given in (49). Note that during the design process, compromises are needed, and sometimes better solutions are obtained by selecting some *non-dynamic* weighting functions. To simplify the design, all of the $2^4$ $H_\infty$ controllers are designed using these weighting functions as inputs in Matlab function "*hinfgs*".

$$\mathbf{W_u}=10^{-7}\mathbf{I}_2,\mathbf{W_e}=\frac{2s+1}{s+0.0001}\mathbf{I}_4,\mathbf{W_d}=10^{3}\mathbf{I}_2,\mathbf{W_n}=10^{6}\mathbf{I}_4 \qquad (49)$$

IV.4. *Results – Comparison*

Fig. 3a shows the commanded joint trajectories and the joint responses, when applying the MB- PD, the MB-PD/ $H_\infty$ and the LPV/ $H_\infty$ control laws. The MB-PD joint response differs significantly from the desired one due to parameter uncertainties and disturbances. Improved trajectory tracking is achieved using both the MB – PD/ $H_\infty$ and the LPV/ $H_\infty$ controllers, while the corresponding torques are at the same level in all three cases, see Fig. 3b. However, the torques generated by the LPV/ $H_\infty$ controller are much noisier than the others since the design of each of the $2^4$ $H_\infty$ controllers using the weighting functions given by (49) may not be suitable for all these controllers and therefore not be robust to noise rejection. To improve this, a redesign of each $H_\infty$ controller is required making the design of the LPV/ $H_\infty$ controller even more complex. The corresponding tracking error responses (noise not shown) of the MB-PD/ $H_\infty$ and the LPV/ $H_\infty$ are shown in Fig. 4.

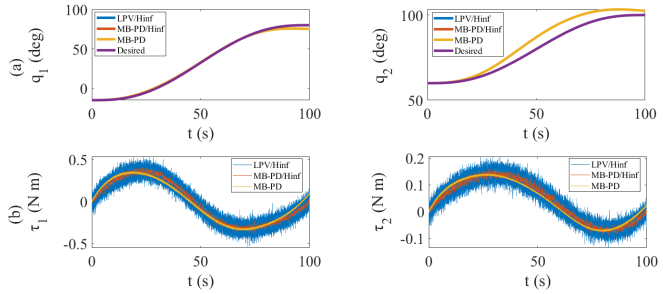


Fig. 3. (a) Desired and joint trajectories for (i) MB-PD Control, (ii) MB-PD/ $H_\infty$ Control, (iii) LPV/ $H_\infty$ Control and (b) Required torques.

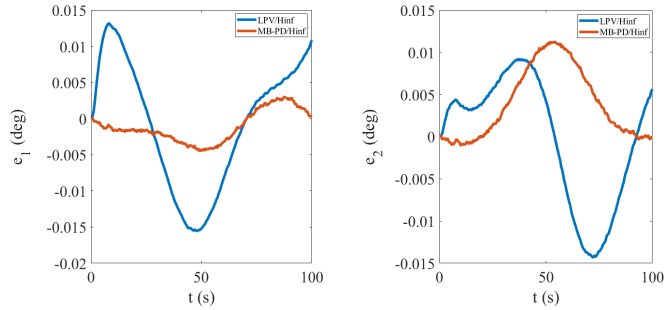


Fig. 4. Error response (noise not shown) for (i) MB-PD/ $H_\infty$ and (ii) LPV/ $H_\infty$ Controllers.

Also, the MB – PD/ $H_\infty$ response is better than the response of LPV/ $H_\infty$, considering both the errors and the required joint torques, as can be seen in Fig. 3b and 4. Fig. 5 shows some snapshots of the SMS motion in SimScape environment in case the MB – PD/ $H_\infty$ is applied.

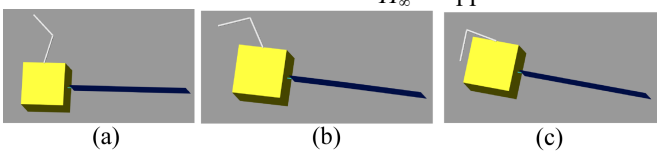


Fig. 5. Snapshots of the SMS in the Simscape© environment. (a) Initial, (b) Intermediate and (c) Final manipulator configuration.

Due to implementation and real-time requirements, low computational complexity is needed for each controller. Table III, displays the mean value of the computational effort, as indicated by the time (ms) required to run a single control loop in a PC with 6-Core 3.59 GHz Processor and 16.0 GB RAM; this time is of the same order for all three controllers.

TABLE III. COMPUTATIONAL EFFORT OF CANDIDATE CONTROL LAWS.

| **Candidate Controller** | **MB- PD** | **MB-PD/ $H_\infty$** | **LPV/ $H_\infty$** |
|---|---|---|---|
| **Computational Effort (ms)** | 7.25 | 8.92 | 8.15 |

In Table IV, an evaluation of the candidate controllers is presented, using the employed selection criteria. Considering the total performance, one can conclude that the model-based MB-PD/ $H_\infty$ controller is the most promising. It is as effective as the LPV/ $H_\infty$ and its design can be extended easily to real spatial SMS; this is unlike the LPV design whose extension in real spatial SMS is not a trivial task.

TABLE IV. CONTROL LAWS COMPARISON - SELECTION CRITERIA.

| **Candidate Controller** | **MB-PD** | **MB-PD/ $H_\infty$** | **LPV/ $H_\infty$** |
|---|---|---|---|
| **Design Complexity** | + + | + | - |
| **Trajectory Errors** | - | + + + | + + |
| **Required Torques** | + + | + + | + |
| **Computational Effort** | + + + | + | + + |
| **Total Performance** | + + + + + + | + + + + + + + | + + + + |

## V. CONCLUSION

The design of LPV controllers for SMS is not a trivial task even for simple planar manipulators; no systematic approach exists for the selection of the appropriate scheduling parameters, limiting their application to real spatial SMS. In this work the effectiveness of the LPV controller against alternative model-based controllers was studied aiming at their applicability to realistic systems. An *LPV plus* $H_\infty$ controller is compared to *Model-Based PD*, and *Model-Based PD plus* $H_\infty$ controllers considering their robustness to parametric uncertainty, noisy measurements, and disturbances due to solar panel and fuel sloshing. The employed criteria included: (i) Design Complexity, (ii) Trajectory Errors, (iii) Required Torques, and (iv) Computational Effort. It was found that the *Model – Based PD plus* $H_\infty$ controller is the most promising since it is as effective as the LPV/ $H_\infty$ control law, while its design can be extended easily to real spatial SMS. This is unlike the LPV control design whose extension in real spatial SMS is not straightforward.

## REFERENCES


[1] Papadopoulos, E., Aghili, F., Ma, O., and Lampariello, R. "Robotic Manipulation and Capture in Space: A Survey," *Frontiers: Robotics & AI - Space Robotics*, 9, July 2021.

[2] Nanos, K., Xydi-Chrysafi, F., and Papadopoulos, E., "On Impact Deorbiting for Satellites Using a Prescribed Impedance Behavior," *IEEE 58th Conference on Decision and Control,* Nice, France, Dec. 11-13, 2019, pp. 2126 – 2131.

[3] Rotondo, D., Nejjari, F., and Puig, V., "Model reference quasi-LPV control of a quadrotor UAV," *IEEE Conference on Control Applications* (*CCA*), Juan Les Antibes, France, Oct. 2014, pp. 736–741.

[4] Corti, A., Dardanelli, A., and Lovera, M., "LPV Methods for Spacecraft Control: An Overview and Two Case Studies," *IEEE American Control Conference* (*ACC*), Montreal, QC, Canada, June 27 – 29, 2012, pp. 1555 – 1560.

[5] Hashemi, S. M., Abbas, H. S., Werner, H., "Low-complexity Linear Parameter-varying Modeling and Control of a Robotic Manipulator," *Control Engineering Practice*, 20, 2012, 248–257.

[6] Hoffmann, C., Hashemi, S.M., Abbas, H. S., and Werner, H., "Benchmark Problem — Nonlinear Control of a 3-DOF Robotic Manipulator," *IEEE Conference on Decision and Control (CDC)*, December 2013.

[7] Sun, Y., Xu, F., Wang, X., and Liang, B., "LPV Model-based Gain-scheduled Control of a Space Manipulator," *IEEE Conference on Decision and Control (CDC)*, Miami Beach, FL, USA, Dec. 17-19, 2018, pp. 5114-5120.

[8] Kraïem, S., Rognant, M., Biannic, JM. and Brière, Y., "Dynamics and robust control of a space manipulator with flexible appendages for on-orbit servicing," *CEAS Space J*, (2022).

[9] Nanos, K., and Papadopoulos, E., "On Cartesian Motions with Singularity Avoidance for Free-floating Space Robots," *IEEE International Conference on Robotics and Automation* (*ICRA'12*), May 14–18, 2012, St. Paul, MN, USA, pp. 5398-5403.

[10] Nanos, K., and Papadopoulos, E. "On the Dynamics and Control of Free-floating Space Manipulator Systems in the Presence of Angular Momentum," *Frontiers: Robotics & AI - Space Robotics*, 4:26, 2017.

[11] Leissa, A. W., "The free vibration of rectangular plates," *Journal of Sound and Vibration*, 31, 1973, pp. 257-293.

[12] Christidi-Loumpasefski, O., Rekleitis, G., Papadopoulos, E., and Ankersen, F., "On System Identification of Space Manipulator Systems Including their Fuel Sloshing Effects," *IEEE Robotics and Automation Letters (RA-L)*, Volume: 8, Issue: 5, May 2023, pp. 2446 – 2453.

[13] Anastasiou, D., Nanos, K., and Papadopoulos, E., "Robust Model-based Control for Free-floating Space Manipulator Cartesian Motions," *30th Mediterranean Conference on Control and Automation* (*MED '22*), Vouliagmeni, Greece, June 28-July 1, 2022.

[14] Zhou, K., and Doyle, J.C., Essentials of Robust Control. *Prentice Hall*, New Jersey, 1998.

[15] Armstrong, B., "On Finding Exciting Trajectories for Identification Experiments Involving Systems with Nonlinear Dynamics," *International J. of Robotics Research*, v. 8, n. 6, December 1989, pp. 28-48.

[16] Nanos, K., and Papadopoulos, E., "On Parameter Estimation of Space Manipulator Systems with Flexible Joints Using the Energy Balance," *IEEE International Conference on Robotics and Automation (ICRA '19)*, Montreal, Canada, May 20-24, 2019, pp. 3570-3576.